Supplementary Information

Facile spray reaction synthesis and characterization of hierarchically porous SnO_2 microspheres for enhanced dye-sensitized solar cell

Hui Zhang,[*a] Rong Wu,[a] Hong Xu,[a] Fan Li,[*b] Shuo Wang,[a] Jinshu Wang,[*c] and Tingting Zhang[a†]

[a.] School of Science, Beijing Jiaotong University, Beijing 100044, PR China. E-mail: hzhang1@bjtu.edu.cn
[b.] College of Environmental and Energy Engineering, Beijing University of Technology, Beijing 100124, PR China. E-mail: vanadiumli@bjut.edu.cn
[c.] College of Materials, Beijing University of Technology, Beijing 100124, PR China. E-mail: wangjsh@bjut.edu.cn

Table of contents

1. Figures and tables

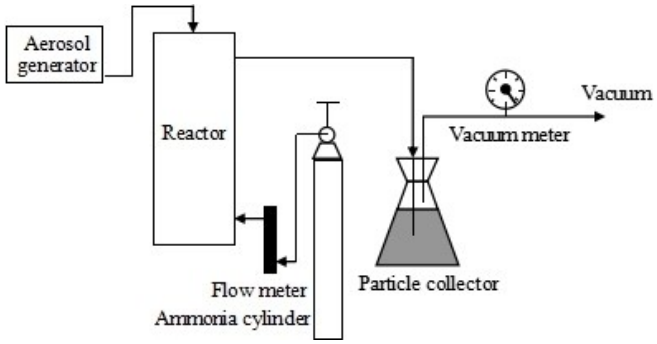

Figure S1. Schematic set-up for spray reaction process.

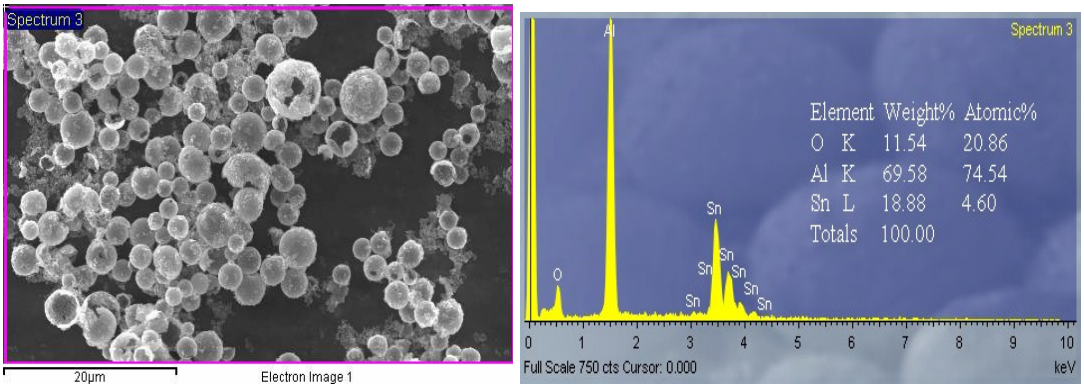

Figure S2. Representative EDX spectrum (right) of synthesized SnO2 spheres (left).

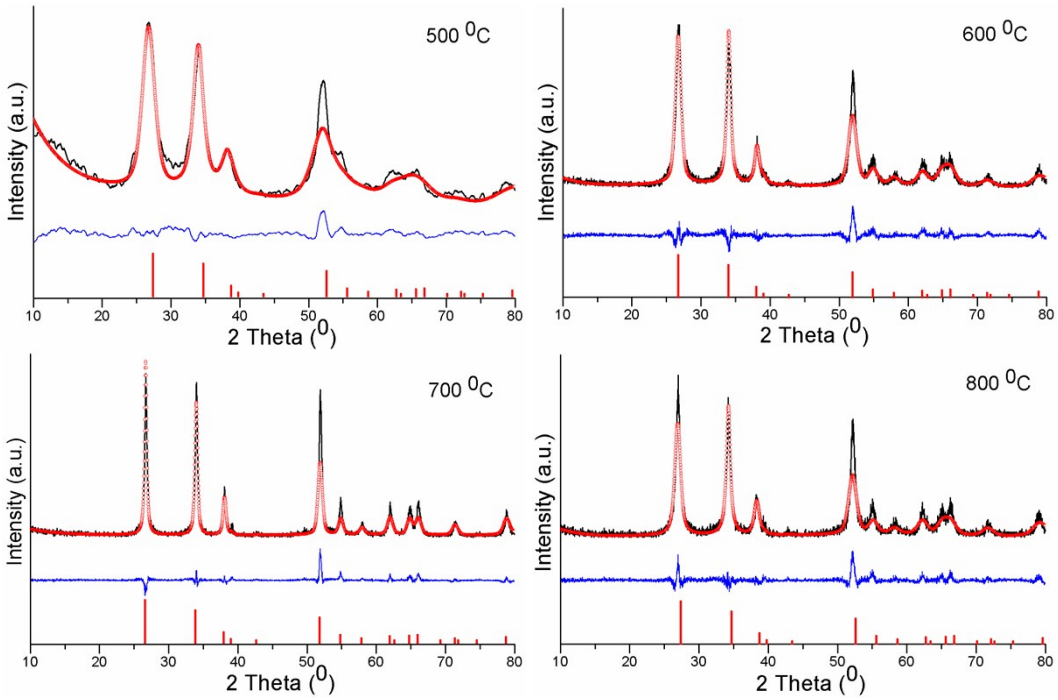

Figure S3. Rietveld-refined XRD patterns of SnO_2 porous spheres calcined at 500-800 °C: ─Experimental pattern, Refined pattern, ─ difference pattern, | (h k l) lines.

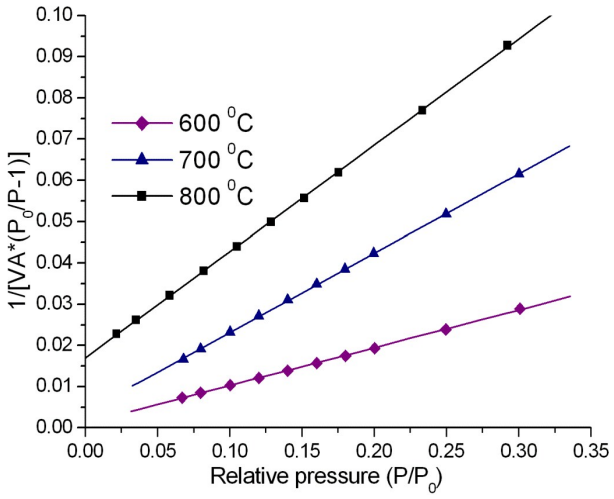

Figure S4. BET plots of SnO_2 porous spheres calcined at 600-800 °C.

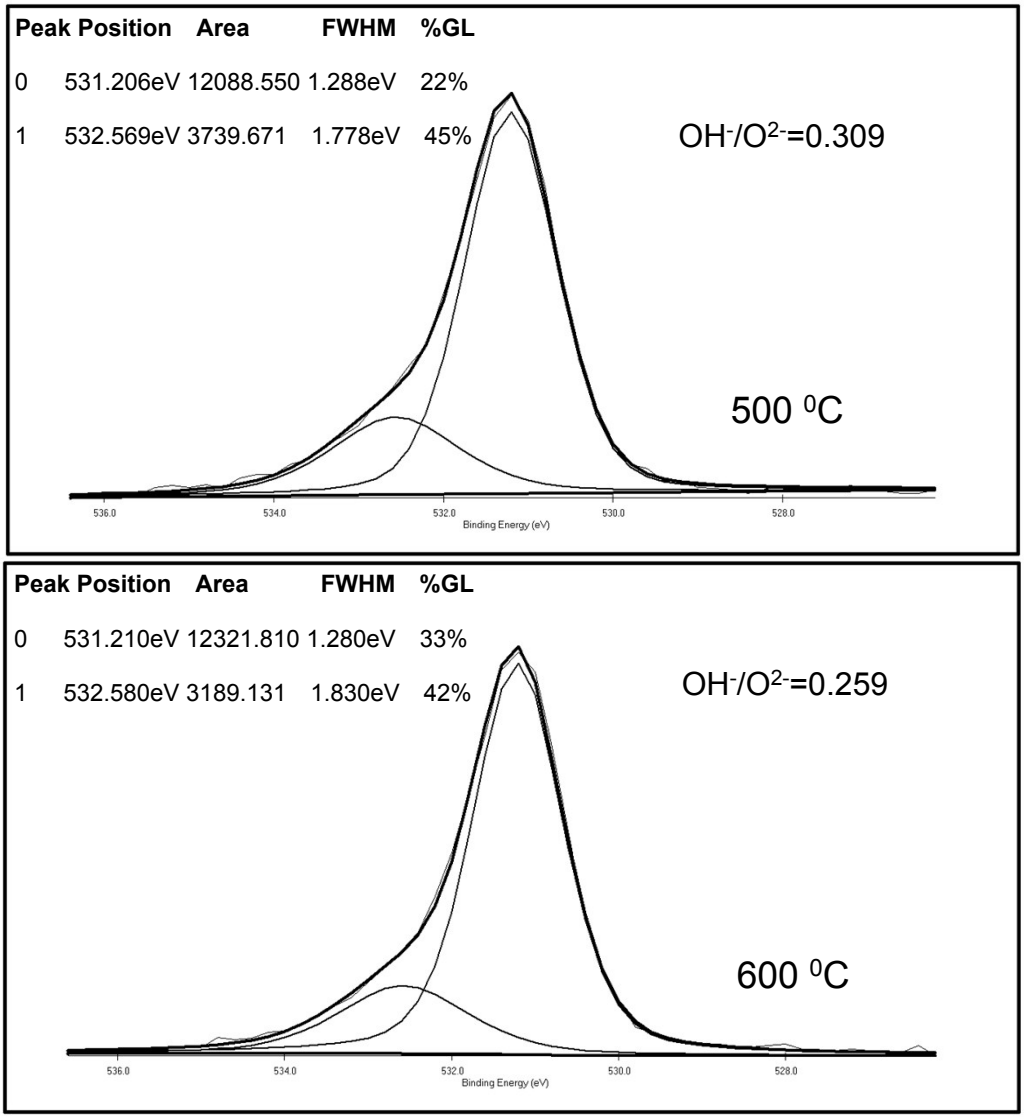

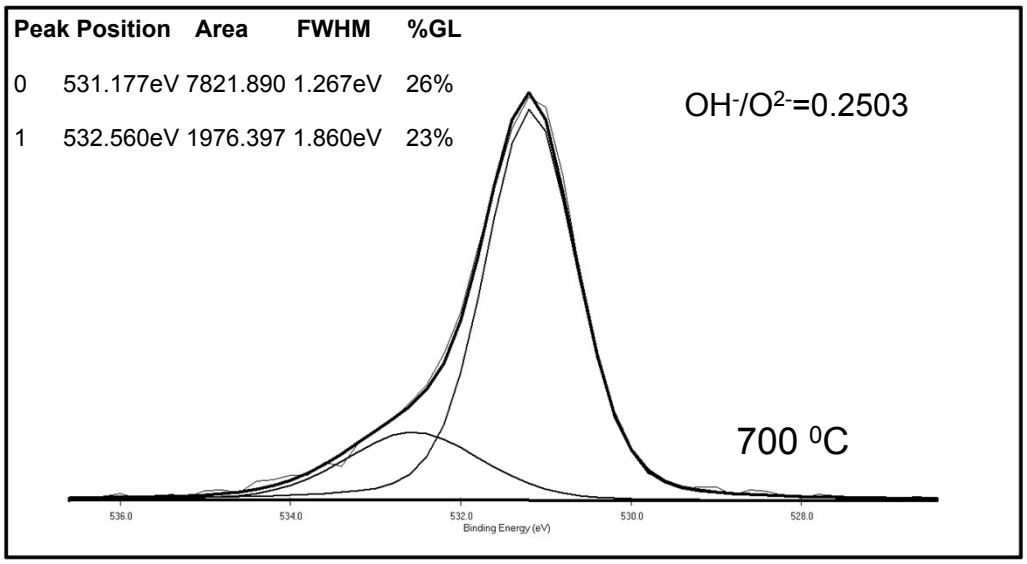

Figure S5. The fitting results of O1s XPS spectra measured for SnO_2 spheres annealed at 500-700 °C.

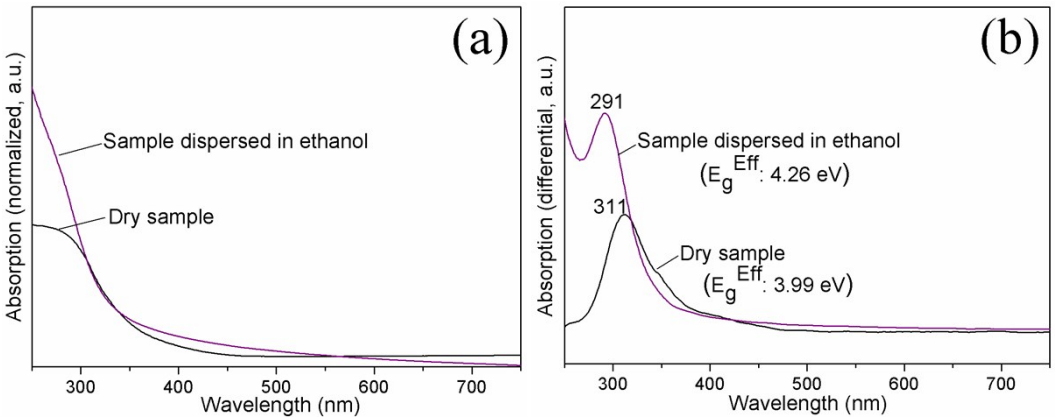

Figure S6. (a) UV-Vis absorption spectra and corresponding differential absorption spectra of the dry 600 °C SnO_2 spheres and the 600 °C SnO_2 spheres dispersed in ethanol.

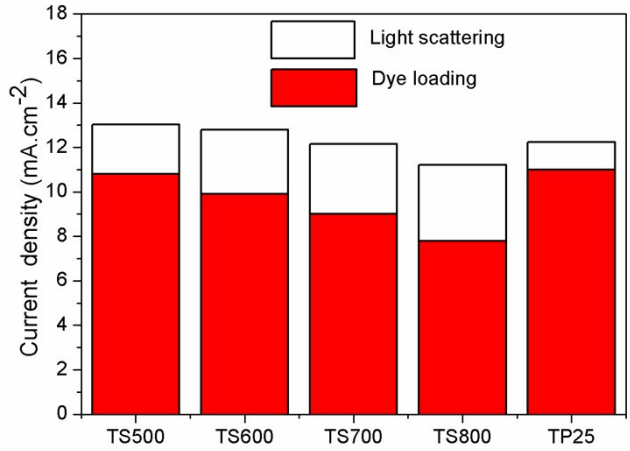

Figure S7. Histogram for the contributions to current density of dye loading and light scattering capability.

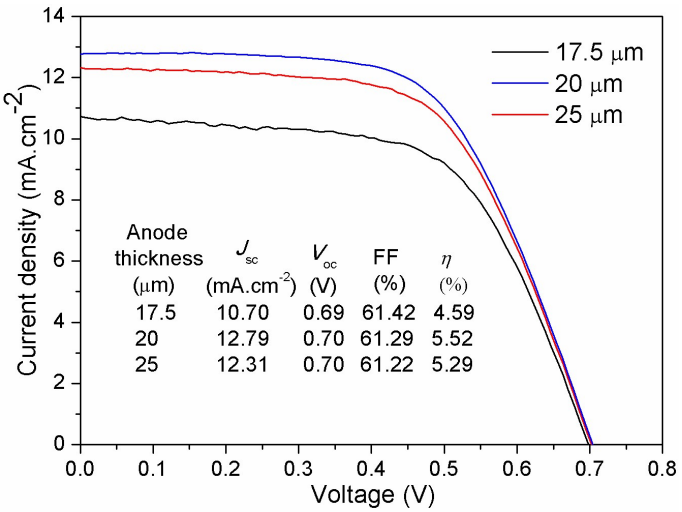

Figure S8. I-V curves for cells with different anode thickness using SnO_2 microspheres heated at 600 °C as scattering layer.

Table S1. Assignment of the Bands in FTIR Spectra of N719, N719-P25, and N719-S500.

N719 ν(cm^{-1})	N719-S500 ν(cm^{-1})	N719-P25 ν(cm^{-1})	Assignment
1232	1237	1266	C-O
1373	1377	1382	COO^-_{sym}
1404	1408	1430	bpy
1468	1461	1469	δ(CH_2) in TBA
1546	1541	1560	bpy
1607	1621	1610	COO^-_{asym}
1712	1713	1693	C=O
2101	—	2079	NC
2875	2874	2852	$CH_{2,\ asym}$
2933	2930	2922	$CH_{2,\ sym}$
2963	2965	2971	CH_3

Table S2. Summary of Δν Values for Carboxylate/Carboxylic Acid Group-SnO2/TiO2 System Compounds.

Compound	ν_{asym}(COO) (cm^{-1})	ν_{sym}(COO) (cm^{-1})	Δν (cm^{-1})	Binding mode
N719	1607	1373	234	N/A
N719-S500	1621	1377	244	Unidentate
N719-P25	1610	1382	228	Bridging

2. Calculation for the SnO_2 effective band gap energy (E_g^{eff})

When the SnO_2 crystallite radius is near or larger than the exciton Bohr radius (2.7 nm) of bulk SnO_2, E_g^{eff} of SnO_2 crystallite can be approximately calculated by following equation.

$$E_g^{eff} \approx E_g^{bulk} + \frac{\hbar^2 \pi^2}{2\mu R^2} \quad (1)$$

where E_g^{bulk} is the bulk band gap energy, R is the crystallite radius, ħ is the reduced Planck constant, μ is the effective reduced mass ($\mu \approx 0.275 m_e$).